2005 American Control Conference
June 8-10, 2005. Portland, OR, USA

Stability Analysis of PID Controllers for Integral Processes with Time Delay

Linlin Ou, Youchun Tang, Danying Gu, and Weidong Zhang

Abstract—**In this paper, the problems of stabilizing integral plants with time delay using the classical proportional-integral-derivative (PID) controllers and the practical single-parameter (containing only one adjustable parameter) PID controllers are considered, respectively. The complete set of stabilizing parameters of the classical PID controller for the integral plant with time delay and time constant is determined using the extended Hermite-Biehler Theorem applicable to quasi-polynomials. Owning to the difficulty in analyzing the complex closed-loop characteristic equation based on the extended Hermite-Biehler Theorem, a simple method called dual-locus diagram, is adopted to present the stabilizing region of the practical single-parameter PID controller.**

I. Introduction

INTEGRAL plants with time delay are frequently encountered in industrial process control. Generally, these integral processes are modeled as $ke^{-\theta s}/s$ or $ke^{-\theta s}/[s(\tau s+1)]$ for the purpose of controller design. The combined effect of the poles at the original point and the delay lead to great difficulty in controller design and system stability [1]. PID control remains the most popular approach for industrial process control. Thus, it is of great significance to solve the stability problem of PID controller and to find new design methods leading to the optimal operation of PID controllers for integral processes with time delay. Morari [2] and Zhang [3, 4] presented two kinds of single-parameter PID controllers analytically for integral processes with time delay: H_2 PID controller and H_∞ PID controller. These controllers can provide quantitative time-domain and frequency-domain responses.

Since the minimal requirement for PID controllers is to make the system stable, it is desirable to know the complete set of the stabilizing PID controller parameter for a given plant before controller design and tuning. However, it is not a trivial task to analyze the stability of plants with time delay. Recently, using the extended Hermite-Biehler Theorem, the complete PID stability regions for first-order plants with time delay have been derived [5]. Whereas, the results are not applicable to integral plants with time delay and time constant since the plants are of second order. The D-partition technique has been used to construct the complete set of the stabilizing PID controller parameters for first-order plus dead-time unstable processes [6], but the results cannot imply that the determination of the stabilizing region of the proportional gain is independent of the integral and derivative gains. Moreover, this method requires a change in the time scale and is not applicable to high-order plants. Although the method of PID stabilization for general plants with time delay has been developed [7], the stabilizing set of the proportional gain of PID controller cannot be determined. Furthermore, for integral plants with time delay and time constant, taking the approach cannot present the complete stabilizing set in the space of the integral and derivative gains since there is no corresponding ω value to make $L(\omega)$ in the crucial equation (35) (in [7]) equivalent to the delay L_0. Thus, in this paper, the stabilizing problem of the classical PID controller for integral processes with time delay and time constant is analyzed on the basis of the Hermite-Biehler Theorem. The range of the admissible proportional parameter is first determined. The set of stabilizing integral and derivative constant values are then derived.

The single-parameter PID controllers are suboptimal and easy to use. However, they are designed based on Pade approximation, indicating that they may fail to stabilize the original plant in spite of their absolute stabilization for the approximated plants. In order to stabilize the original integral process, certain constraints must be imposed on the only adjustable parameter. Because of the complexity of the resulting closed-loop characteristic equation, it is relatively difficult to derive the exact stabilization range for the adjustable parameter based on the Hermite-Biehler Theorem. Though the method developed by Xu [7] can be used to compute the stabilizing region, the analytical results and the relationship between the stabilizing region and the plant parameters are not be derived. The dual-locus diagram method is used in this paper to analyze the stabilizing problem of the single-parameter PID controller for integral processes with time delay. It employs a counterclockwise unit circle and requires only the plotting of a simple curve derived from the open-looped transfer function free of delay.

Manuscript received September 10, 2004. This work is supported by National Natural Science Foundation of China (60274032), SRFDP (20030248040), and Science and Technology Rising-Star program of Shanghai (04QMH1405).

Linlin Ou is with the Department of Automation, Shanghai Jiaotong University, Shanghai, 200030, P. R. China. (e-mail: oulinlin@sjtu.edu.cn).
Youchun Tang is with the College of Management, Shanghai University of Engineering Science.
Danying Gu and Weidong Zhang are with the Department of Automation, Shanghai Jiaotong University, Shanghai, 200030, P. R. China. (e-mail: wdzhang@sjtu.edu.cn).

0-7803-9098-9/05/$25.00 ©2005 AACC

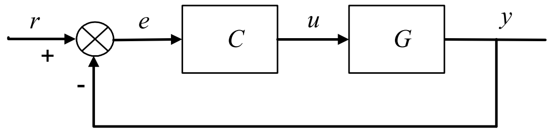

Fig. 1. Feedback control system

II. STABILITY ANALYSIS OF CLASSICAL PID CONTROLLER

The integral process with time delay and time constant is described as the following transfer function,

$$G(s)=\frac{k}{s(\tau s+1)}e^{-\theta s} \quad (1)$$

where k, τ and θ are assumed to be positive. Consider the unity feedback control system in Fig.1, where $C(s)$ is the controller, $G(s)$ is the plant to be controlled, r is the setpoint, and y is the output of the plant. If $C(s)$ in Fig.1 is the PID controller with the transfer function,

$$C(s)=k_p+\frac{k_i}{s}+k_d s \quad (2)$$

the characteristic equation of the closed-loop system is

$$\delta(s)=s^2(\tau s+1)+(kk_i+kk_p s+kk_d s^2)e^{-\theta s} \quad (3)$$

A. The Extension of the Hermite-Biehler Theorem

For a linear time invariant system with time delay the characteristic equation can be written as

$$f(s)=\sum_{j=1}^{n}e^{s\lambda_j}P_j(s) \quad (4)$$

where $P_j(s)$ for $j=1,\cdots,n$ is an arbitrary polynomial, and the λ_j 's are real numbers satisfy $\lambda_1<\lambda_2<\cdots<\lambda_n$, $|\lambda_1|<\lambda_n$. Function (4) is called a quasi-polynomial [8]. $f_r(\omega)$ and $f_i(\omega)$ denote the real and imaginary parts of $f(j\omega)$ respectively, i.e. $f(j\omega)=f_r(\omega)+jf_i(\omega)$.

The extended Hermite-Biehler Theorem to study the stability of quasi-polynomial (4) is stated as follows [9]:

Theorem 2.1 $f(s)$ is stable if and only if

1) $f_r(\omega)$ and $f_i(\omega)$ have only real roots and these roots interlace,

2) $f_i'(\omega^*)f_r(\omega^*)-f_i(\omega^*)f_r'(\omega^*)>0$ for some $\omega^*\in(-\infty,+\infty)$, where $f_r'(\omega)$ and $f_i'(\omega)$ denote the first derivative with respect to ω of $f_r(\omega)$ and $f_i(\omega)$, respectively.

To make sure that $f_r(\omega)$ and $f_i(\omega)$ have only real roots, the following theorem is introduced [9, 10]:

Theorem 2.2 Let p and q denote the highest powers of s and e^s respectively in $f(s)$. Let ε be a constant such that the coefficients of terms of highest degree in $f_r(\omega)$ and $f_i(\omega)$ do not vanish at $\omega=\varepsilon$. Then the necessary and sufficient condition that $f_r(\omega)=0$ or $f_i(\omega)=0$ has only real roots is that: in the strip $-2l\pi+\varepsilon\le\omega\le 2l\pi+\varepsilon$, $f_r(\omega)$ or $f_i(\omega)$ has exactly $4lq+p$ real roots starting with a sufficiently large l.

B. Stabilization Scope of the Classical PID Controller

The open-looped transfer function is written as:

$$H(s)=G(s)C(s)=\frac{N(s)}{D(s)}e^{-\theta s}$$

Where $N(s)$ and $D(s)$ represent real polynomials of degree m and n, respectively.

First of all, in order to make the closed-loop system with time delay stable, the following two necessary requirements must be satisfied [7]:

1) $n>m$, or, $|b_m/a_n|<1$ for $n=m$, where a_n and b_m are leading coefficients of $D(s)$ and $N(s)$, respectively.

2) The corresponding delay-free closed-loop system is stable.

For the integral plant (1) and the classical PID controller (2), the system shown in Fig.1 satisfies requirement 1 since $n>m$ ($n=3$ and $m=2$). Then, requirement 2 is analyzed. For the integral plant free of delay, the closed-loop characteristic equation is given by

$$\delta(s)=s^2(\tau s+1)+(kk_i+kk_p s+kk_d s^2)$$

Using the Routh-Hurwitz criterion to determine closed loop stability, the following inequalities must hold:

$$k_p>0,\ k_i>0,\ k_p+kk_dk_p-\tau k_i>0 \quad (5)$$

Convert the characteristic function (3) into the following quasi-polynomial:

$$f(s)=\delta(s)e^{\theta s}=kk_i+kk_p s+kk_d s^2+s^2(\tau s+1)e^{\theta s} \quad (6)$$

Since $e^{\theta s}$ has not any finite zeros, the zeros of $\delta(s)$ are identical to those of $f(s)$. Then, the stability of the system with characteristic equation (6) is equivalent to the condition that all the zeros of $f(s)$ are in the open left-half plane. Substituting $s=j\omega$ into (6) and taking $z=\theta\omega$ yield

$$f_r(z)=kk_i-kk_d z^2/\theta^2-z^2\cos(z)/\theta^2+\tau z^3\sin(z)/\theta^3 \quad (7)$$

$$f_i(z)=kk_p z/\theta-z^2\left[\tau z\cos(z)/\theta+\sin(z)\right]/\theta^2 \quad (8)$$

Secondly, Theorem 2.2 is used to obtain the requirement that $f_i(z)$ has only real roots. We choose $\varepsilon=\pi/3$ to satisfy the condition that $\sin(\varepsilon)\ne 0$. Substituting $s_1=\theta s$ into (6), it is seen that for the new quasi-polynomial in s_1, $p=3$ and $q=1$. From (8) it is known that one root of the imaginary part is $z_0=0$ and the other roots are given by

$$kk_p-\tau z^2\cos(z)/\theta^2-z\sin(z)/\theta=0 \quad (9)$$

Equation (9) can be rewritten as

$$[kk_p-\tau z^2\cos(z)/\theta^2]/\sin(z)=z/\theta \quad (10)$$

It is difficult to be solved analytically. However, the nature of the solution can be examined graphically by plotting the left and right terms of equation (10). We sketch $[kk_p-\tau z^2\cos(z)/\theta^2]/\sin(z)$ and z/θ to obtain the plot shown in Fig.2. Fig. 2(b) is the local enlarged image of Fig. 2(a). Denote $[kk_p-\tau z^2\cos(z)/\theta^2]/\sin(z)$ by $L(z)$. The plot in Fig. 2(b) corresponds to the case where $0<k_p<k_u$ and k_u is the value that makes the line z/θ tangent to the plot of $L(z)$. Since $L(z)$ is an odd function of z, it is seen from Fig.2 that only if the line z/θ intersects the plot of $L(z)$ twice in the interval $(0,\pi)$, $f_i(\omega)$ has exactly $4l+3$ real

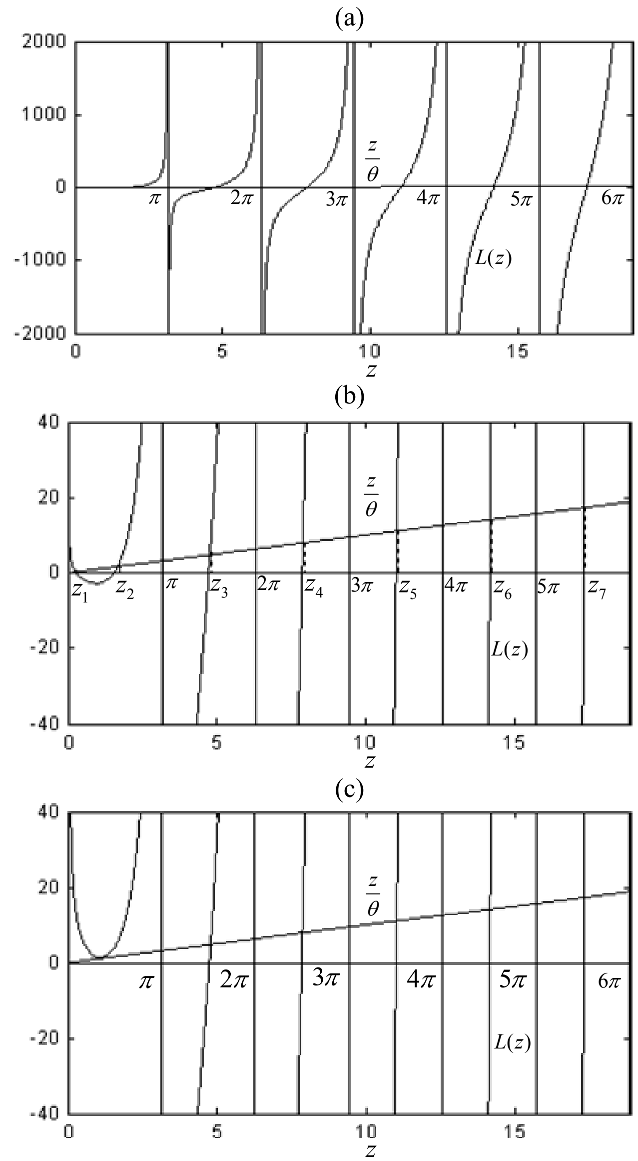

Fig. 2. Plot of the left and right terms involved in equation (10)
(a) $0 < k_p < k_u$. (b) local enlarged image of Fig.2(a). (c) $k_p = k_u$.

roots in the interval $[-2l\pi + \pi/3,\ 2l\pi + \pi/3]$ for $l = 1, 2, \cdots$, including a root at the origin. If k_p increases to a enough large value, the line z/θ and the plot of $L(z)$ will have only one intersection or no intersection in the interval $(0, \pi)$, leading to the number of the real roots of $f_i(z)$ not satisfying Theorem 2.2 and thereby ruling out closed-loop stability. The upper bound k_u on the allowable value of k_p is determined according to the case of Fig. 2(c), i.e. the line z/θ is tangent to the plot of $L(z)$ in the interval $(0, \pi)$. Denote by β the value of z for which this intersection occurs. Then, the following set of equations can be obtained

$$[kk_u\theta^2 - \tau\beta^2\cos(\beta)]/[\theta^2\sin(\beta)] = \beta/\theta \tag{11}$$

$$\frac{d}{dz}\{[kk_u\theta^2 - \tau z^2\cos(z)]/[\theta^2\sin(z)]\}_{z=\beta} = 1/\theta \tag{12}$$

Eliminating kk_u in equations (11) and (12), we yield the value of β in the interval $(0, \pi)$ from the following equation:

$$tg(\beta) = \frac{2\tau\beta + \beta\theta}{\tau\beta^2 - \theta} \tag{13}$$

If we substitute the resultant value of β into (11), k_u is obtained as:

$$k_u = \frac{1}{k}\left[\frac{\tau\beta^2}{\theta^2}\cos(\beta) + \frac{\beta}{\theta}\sin(\beta)\right]$$

Since the minimal requirement (5) to make the system in Fig.1 stable implies that $k_p > 0$, the imaginary part of $f(s)$ has only simple real roots if and only if

$$0 < k_p < \frac{1}{k}\left[\frac{\tau\beta^2}{\theta^2}\cos(\beta) + \frac{\beta}{\theta}\sin(\beta)\right] \tag{14}$$

Thirdly, consider the condition that $f_r(\omega)$ has only real roots and these roots interlace with that of $f_i(\omega)$ in Theorem 2.1. The real part $f_r(z)$ in (7) is rewritten as

$$f_r(z) = \frac{kz^2}{\theta^2}(-k_d + m(z)k_i + b(z)) \tag{15}$$

where
$$m(z) = \frac{\theta^2}{z^2} \tag{16}$$

$$b(z) = -\frac{1}{k}\cos(z) + \frac{\tau z}{k\theta}\sin(z) \tag{17}$$

For $z_0 = 0$, using (7) yields:

$$f_r(z_0) = kk_i$$

In view of the stability requirement $k_i > 0$ for the delay-free case in (5), it is known that $f_r(z_0) > 0$. The condition that the roots of $f_r(z)$ interlace with those of $f_i(z)$ indicates:

$$f_r(z_1) < 0, f_r(z_2) > 0, \cdots f_r(z_{2j-1}) < 0, f_r(z_{2j}) > 0$$

where $j = 1, 2, 3\cdots$, z_1, z_2, z_3, z_{2j-1} and z_{2j} are the positive real roots of (8) arranged in increasing order of magnitude. Since $f_r(z)$ is an even function, the negative-real values of z are not considered. Thus,

$$(-1)^j k_d < (-1)^j m(z_j)k_i + (-1)^j b(z_j),\ j = 1, 2, 3\cdots \tag{18}$$

The intersection of all these regions in the $k_i - k_d$ space is exactly the set of (k_i, k_d) for which the roots of $f_r(z)$ and $f_i(z)$ interlace for a given admissible value of k_p. The boundaries are determined by the following equations:

$$k_d = m(z_j)k_i + b(z_j) \quad \text{for } j = 1, 2, 3\cdots \tag{19}$$

It is known from Equation (16), $m(z) > 0$, $m(z_j) > m(z_{j+1})$, and $m(z_j) \to 0$ as $j \to \infty$. The change of $b(z_j)$ is difficult to be found with the theoretical approach, so it is examined with the graphic approach. Given a stabilizing k_p value satisfying (14), the intersections of the curves $\tau[kk_p - \tau z^2\cos(z)/\theta^2]/k$ and $\tau z\sin(z)/\theta k$ are plotted in Fig.3 to obtain the real roots of equation (9), denoted by $z_1, z_2, z_3\cdots$. Fig. 3(b) is the enlarged image of Fig. 3(a). It is observed that, for the odd roots of (9), the corresponding $\tau z\sin(z)/\theta k$ is decreasing by large magnitude, and for the even ones, the corresponding $\tau z\sin(z)/\theta k$ is increasing by

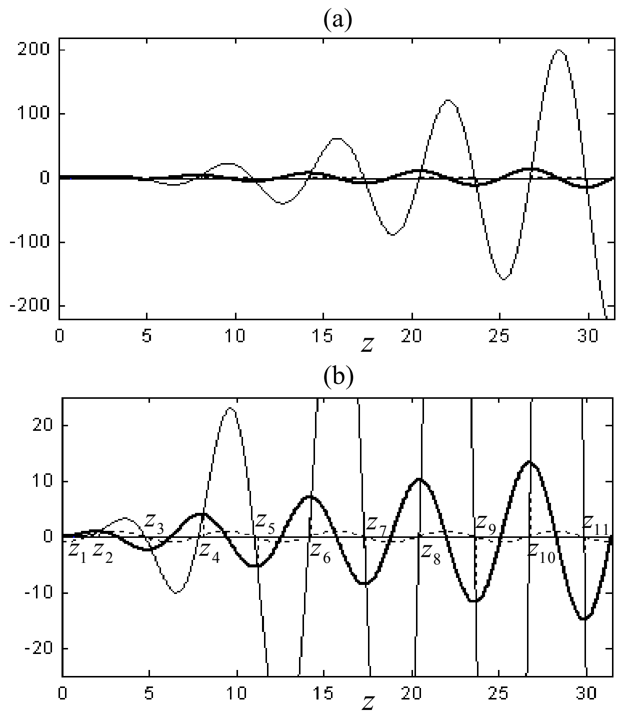

Fig.3. plots of $\tau(kk_p - \tau z^2 \cos(z)/\theta^2)/k$ (thin solid line), $\tau z \sin(z)/\theta k$ (thick solid line) and $-\cos(z)/k$ (dotted line)

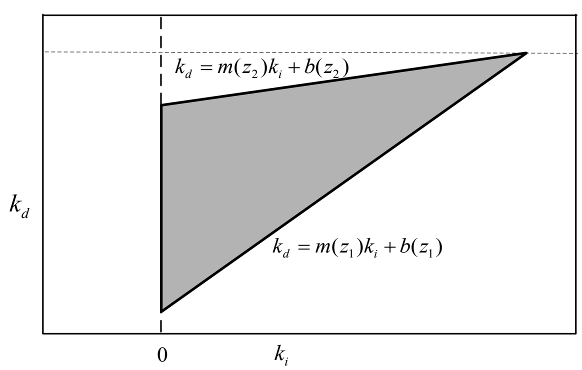

Fig.4. Stabilizing region of (k_i, k_d) for the admissible k_p

large magnitude. However, compared to the change of $\tau z_j \sin(z_j)/\theta k$, the difference between the values of $-\cos(z_{j+2})/k$ and $-\cos(z_j)/k$ is much smaller both for odd and even j. Thus, $b(z_j)$ in (17) have the similar change rules as $-\tau z_j \sin(z_j)/\theta k$, i.e.

1) $b_j > b_{j+2}$ and $b_j \to -\infty$ as $j \to \infty$ for odd values of j,

2) $b_j < b_{j+2}$ and $b_j \to +\infty$ as $j \to \infty$ for even values of j.

Denote as $k_i(z_1, z_{2j})$ the abscissa value of the intersection of the lines $k_d(z_1)$ and $k_d(z_{2j})$. In terms of (19), we know that $k_i(z_1, z_{2j}) = [b(z_{2j}) - b(z_1)]/[m(z_1) - m(z_{2j})]$ .Though the values of $b(z_{2j}) - b(z_1)$ and $m(z_1) - m(z_{2j})$ are increasing with j, the ascending magnitude of the former is much larger than that of the latter owing to the change characteristics of $b(z_{2j})$ and $m(z_{2j})$. This makes $k_i(z_1, z_{2j})$ increase with j, since the values of $b(z_{2j}) - b(z_1)$ and $m(z_1) - m(z_{2j})$ are the positive ones. Therefore, in view of the stability requirements (5) that $k_i > 0$ and the behavior of the parameters $b(z_j)$, $m(z_j)$ and $k_i(z_1, z_{2j})$, the triangle cross-intersection P of the stabilizing region in the (k_i, k_d) space is derived (see Fig.4). The values of k_i and k_d corresponding to the point in the shadow region of Fig.4 are certain to satisfy the requirement $k_p + kk_d k_p - \tau k_i > 0$ in (5), the proof of which is based on simply mathematical calculation and is omitted.

Finally, Condition 2 of Theorem 2.1 is checked. Taking $\omega_0 = 0$ yields $f_r'(z_0) = 0$, $f_r(z_0) = kk_i$ and $f_i'(z) = kk_p/\theta$. Then, $E(z_0) = f_i'(z_0) f_r(z_0) - f_i(z_0) f_r'(z_0) = k^2 k_p k_i / \theta > 0$

Consequently, the necessary and sufficient conditions making the closed-looped characteristic equation stable in Theorem 2.1 are satisfied. The complete stabilizing region of the PID controller parameters is given by:

Theorem 2.3 The range of k_p values for which a given integral plant $G(s)$ with transfer function in (1) can be stabilized using the classical PID controller is that $0 < k_p < \left[\tau\beta^2 \cos(\beta)/\theta^2 + \beta \sin(\beta)/\theta\right]/k$, where β is the solution of the equation (13) in the interval $(0, \pi)$. For each k_p in the range, the stabilizing region in the (k_i, k_d) space is presented by the triangle P with known boundaries (see Fig. 4).

III. Stability Analysis of the Single-parameter PID Controller

A. Dual-locus Diagram Method

The dual-locus diagram method is based on the argument principle.

Theorem 3.1 (Argument principle [11]): Let a function f be meromorphic in the domain interior to a positively oriented simple closed contour C, and suppose that f is analytic and nonzero on C. If, counting multiplicities, Z is the number of zeros and P is the number of poles inside C, then the number of times $f(s)$ winds around the origin is

$$n(f(s), 0) = \frac{1}{2\pi} \Delta_C \arg f(s) = Z - P$$

where $\Delta_C \arg f(s)$ represents the variation of the argument of $f(s)$ along the contour C.

The characteristic equation of the closed-loop system is usually written in the form

$$1 + L(s) = 0 \tag{20}$$

where $L(s)$ is the open-looped transfer function without poles in the right-half plane. Since $L(s)$ has no poles on the right-half plane, the number of the right-half plane poles of the closed-loop transfer function is zero (i.e. $P = 0$). Here, the closed contour C is the Nyquist contour. If the characteristic equation (20) is rearranged as

$$L_1(s) = L_2(s) \tag{21}$$

The dual-locus diagram is obtained when s traverses the Nyquist contour. The argument of $L_1(s) - L_2(s)$ is the angle between the vector joining the corresponding points on the Nyquist plots of $L_1(s)$ and $L_2(s)$, and the positive real axis. According to the argument principle, the system is stable (i.e. $Z=0$) if and only if the variation of the argument of $L_1(s)-L_2(s)$ is zero.

For plants with time delay, the characteristic equation may be transformed into the following form,

$$H(s)=-e^{\theta s} \tag{22}$$

where $H(s)$ is the open-looped transfer function without poles in the right-half plane polynomials of degree m and n respectively, and θ is time delay. The dual-locus diagram method is simply illustrated as follows [10,12]:

Corollary 3.1: If the following conditions are satisfied, the system is stable. Otherwise, it is unstable.

1) Provided that $\theta=0$, the system satisfies two principle necessary requirements given in Section II.

2) Either the loci of $H(s)$ and $-e^{\theta s}$ have no intersection or the locus of $H(s)$ arrives at the point of intersection earlier than that of $-e^{\theta s}$ if the two loci intersect.

B. Stabilization Using Single-parameter PID Controllers

If the model of the integral plant with time delay is described as

$$G(s)=\frac{k}{s}e^{-\theta s} \tag{23}$$

$C(s)$ in Fig.1 is chosen as the following single-parameter PID controller [4]

$$C(s)=K_C(1+\frac{1}{T_I s}+T_D s)\frac{1}{T_F s+1} \tag{24}$$

where

$$T_F=\frac{\lambda^2\theta}{2\lambda^2+4\lambda\theta+\theta^2}, \qquad T_I=2\lambda+\frac{3\theta}{2}$$

$$T_D=\frac{(2\lambda+\theta)\theta}{2T_I}, \qquad K_C=\frac{1}{K}\frac{T_I}{\lambda^2+2\lambda\theta+\theta^2/2}$$

λ is the positive adjustable parameter. The characteristic equation of the system in Fig.1 is given by

$$1+\frac{(1+\theta s/2)[(2\lambda+\theta)s+1]}{\theta\lambda^2 s^3/2+(\lambda^2+2\lambda\theta+\theta^2/2)s^2}e^{-\theta s}=0 \tag{25}$$

which is equivalent to

$$H(s)=-e^{\theta s} \tag{26}$$

i.e.

$$H(s)=\frac{(1+\theta s/2)[(2\lambda+\theta)s+1]}{\theta\lambda^2 s^3/2+(\lambda^2+2\lambda\theta+\theta^2/2)s^2} \tag{27}$$

The loci of $H(s)$ and $-e^{\theta s}$ are shown in Fig.5. When ω increases from 0 to $+\infty$, the locus of $-e^{\theta s}$ is the counterclockwise unit circle originating at (-1, 0), and the locus of $H(s)$ is a curve starting at infinity. The locus of $H(s)$ corresponding to $\omega=-\infty\sim 0$ is symmetric with respect to the real axis. Since the transfer function $H(s)$ has two poles at the origin, its Nyquist plot shifts clockwise from π to $-\pi$ with the infinite radius when s changes from $-j0$ to $j0$. Due to the symmetry property of Nyquist plot, the negative values of ω are not considered.

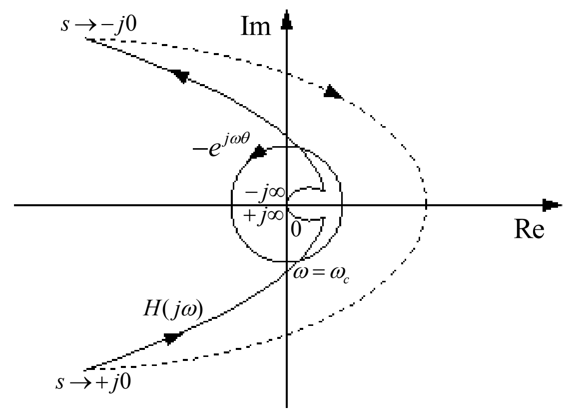

Fig. 5. The loci of $H(j\omega)$ and $-e^{j\omega\theta}$

Firstly, compute the frequency ω_c satisfying the equation

$$|H(j\omega_c)|=\left|\frac{(1+j\omega\theta/2)[j\omega(2\lambda+\theta)+1]}{\theta\lambda^2(j\omega)^3/2+(\lambda^2+2\lambda\theta+\theta^2/2)(j\omega)^2}\right|=1 \tag{28}$$

Simplifying (28) yields

$$a\omega_c^{\,6}+b\omega_c^{\,4}+c\omega_c^{\,2}-1=0 \tag{29}$$

where
$$a=\theta^2\lambda^4/4$$
$$b=(\lambda^2+3\lambda\theta+\theta^2)(\lambda^2+\lambda\theta)$$
$$c=-(4\lambda^2+4\lambda\theta+5\theta^2/4)$$

Equation (29) has six analytical roots, among which the valid solution for ω_c is

$$\omega_c=\sqrt{\sqrt[3]{-\frac{q}{2}+\sqrt{\left(\frac{q}{2}\right)^2+\left(\frac{p}{3}\right)^3}}+\sqrt[3]{-\frac{q}{2}-\sqrt{\left(\frac{q}{2}\right)^2+\left(\frac{p}{3}\right)^3}}-\frac{b}{3a}} \tag{30}$$

where

$$p=\frac{c}{a}-\frac{b^2}{3a^2} \quad \text{and} \quad q=\frac{2b^3}{27a^3}-\frac{bc}{3a^2}-\frac{1}{a}$$

The other five roots are either negative or complex values. Taking $\beta=\lambda/\theta$, we have

$$p=-\left(\frac{16\beta^2+16\beta+5}{\beta^4}+\frac{(\beta^2+3\beta+1)^2(\beta+1)^2}{3\beta^6}\right)\cdot\theta^{-4} \tag{31}$$

$$q=\left[\frac{(\beta^2+3\beta+1)(64\beta^2+64\beta+20)(\beta+1)}{3\beta^7}+\frac{128(\beta^2+3\beta+1)^3(\beta+1)^3}{27\beta^9}-\frac{4}{\beta^4}\right]\cdot\theta^{-6} \tag{32}$$

Thus, the equation (30) can be rewritten as

$$\omega_c=f(\beta)/\theta \tag{33}$$

where $f(\beta)$ denotes the function only relating to β . The phase angle of $H(s)$ at ω_c is

$$\varphi_1=\arctan(\theta\omega_c/2)+\arctan(2\lambda\omega_c+\theta\omega_c)-\arctan(\frac{\theta\lambda^2\omega_c}{2\lambda^2+4\lambda\theta+\theta^2})+\pi \tag{34}$$

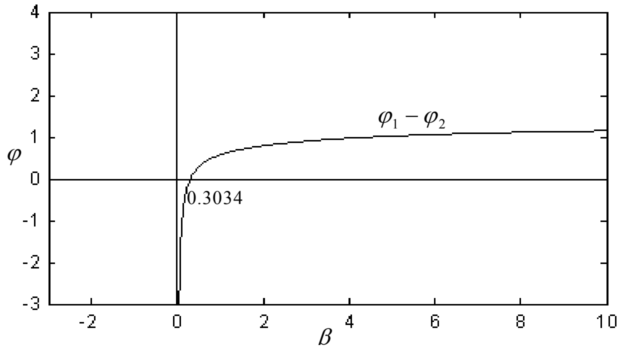

Fig. 6. Plot of $\varphi_1-\varphi_2$ as a function of β

and the phase angle of $-e^{\theta s}$ at ω_c is

$$\varphi_2=\pi+\theta\omega_c \tag{35}$$

From Fig.5, it is seen that the stabilizing condition in Corollary 3.1 can be satisfied only when the phase angle of $H(j\omega)$ at ω_c is larger than that of $-e^{j\omega\theta}$ (i.e. $\varphi_1-\varphi_2>0$). Substituting (30)-(35) and $\lambda=\beta\theta$ into the equation $\varphi_1-\varphi_2=0$, the following equation is obtained.

$$\arctan\left(\frac{f(\beta)}{2}\right)+\arctan(2\beta f(\beta)+f(\beta))-\arctan\left(\frac{\beta^2 f(\beta)}{2\beta^2+4\beta+1}\right)-f(\beta)=0 \tag{36}$$

It is clear that equation (36) is only related to β (i.e. λ/θ). The solution of equation (36) is that $\lambda/\theta=0.3034$. From Fig.6, it is found that the requirement $\varphi_1-\varphi_2>0$ is satisfied only if $\lambda/\theta>0.3034$.

From (27), it is known that the denominator degree of $H(s)$ is larger than its numerator. Using the Routh-Hurwitz criterion, the closed-loop characteristic equation (25) has no right half zeros in the case that $\theta=0$. Moreover, the locus of $H(s)$ arrives at the point of intersection earlier than that of $-e^{\theta s}$ if $\lambda/\theta>0.3034$. Therefore, in order to stabilize the integral plant with the transfer function in (23) using the single-parameter PID controller (24), the value of the adjustable parameter λ must be larger than 0.3034θ in terms of the stability criterions in Corollary 3.1.

For an integral process involving time constant and time delay given by the transfer function (1), the derived practical single-parameter PID controller are [3]:

$$C(s)=K_C(1+\frac{1}{T_I s}+T_D s)\frac{1}{T_F s+1} \tag{37}$$

where

$$T_F=\frac{\lambda^3}{3\lambda^2+3\lambda\theta+\theta^2},\qquad T_I=3\lambda+\theta+\tau$$

$$T_D=\frac{(3\lambda+\theta)\tau}{T_I},\qquad K_C=\frac{1}{K}\frac{T_I}{3\lambda^2+3\lambda\theta+\theta^2}$$

Following similar steps as in the case of the integral plant (23), the range of the adjustable parameter λ for which the single-parameter PID controller (37) can stabilize the integral plant with the transfer function (1) is that $\lambda>0.2291\theta$.

IV. CONCLUSIONS

The complete set of the stabilizing classical PID controller parameters for the integral plant with time delay and time constant has been obtained on the basis of the extended Hermite-Biehler Theorem. The range of the proportional parameter for which a stabilizing PID controller exists is first determined. For a given admissible proportional parameter, the set of stabilizing integral and derivative constant values is shown to be a triangle. Considering the difficulty in analyzing the complex closed-loop characteristic equation based on Hermite-Biehler Theorem and the objective of finding the analytical stabilizing region for the analytical single-parameter PID controller, the dual-locus diagram method is introduced to derive the exact stabilizing range of the adjustable parameter. The derived stabilizing region is analytical and only related to the delay of the plant. The dual-locus diagram method for systems with time delay is simple and effective for the stabilization analysis of the practical single-parameter PID controller. The results in this paper provide insight into the PID stabilization of the integral process with time delay and offer convenience for the tuning of PID controllers.

REFERENCES

[1] J. Marshall, E. H. Gorecki and A. Korytowski, *Time-delay systems: stability and Performance Criteria with Applications*, Ellis Horwood, New York, 1992.

[2] M. Morari and E. Zafiriou, *Robust Process Control*, Prentice-Hall, Englewood Cliffs, NJ, 1989.

[3] W. D. Zhang, X. M. Xu and Y. X. Sun, "Quantitative performance design for integrating processes with time delay", *Automatica*, vol.35, no.4, pp.719-723, 1999.

[4] W. D. Zhang, Y. X. Sun, and X. M. Xu, "PID control for integrator and dead time processes", *ACTA Automatica Sinica*, vol.25, no.4, pp.518-523, 1999.

[5] G. J. Silva, A. Datta and S. P. Bhattacharyya, "New results on the synthesis of PID controllers", *IEEE Transactions on Automatic Control*, vol.47, pp.241-252, 2002.

[6] C. Hwang, J. H. Hwang, "Stabilization of first-order plus dead-time unstable processes using PID controllers", *Control Theory and Applications, IEE Proceedings-*, Vol.151, no.1, pp.89 – 94, 2004.

[7] H. Xu, A. Datta and S. P. Bhattacharyya, "PID stabilization of LTI plants with time-delay", *Proceedings of the IEEE Conference on Decision and Control*, vol.4, no.2, pp.4038-4043, 2003.

[8] V. L. Kharitonov and A. P. Zhabko, "Robust stability of time delay systems", *IEEE Transactions on Automatic Control*, vol.39, no.12, pp.2388-2397, 1994.

[9] R. Bellman and K. L. Cooke, *Differential-Difference Equations*, London, U.K.: Academic, 1963.

[10] L. S. Pontryain, "On the zeros of some elementary transcendental functions", *American Mathematic Society*, vol.2, pp.95-110, 1955.

[11] Y. C. Lin, *Lecture notes on complex variables*, available at http://pc53.math. ntnu.edu.tw/ ~yclin/02a/cx/cx20.pdf, 2002.

[12] Q. C. Zhong, "Robust stability analysis of simple control algorithms in communication networks using dual-locus diagram", *Automatic*, vol.39, no.7, pp.1309-1312, 2003.